RELATIONSHIP OF CALIFORNIA SARDINE (*SARDINOPS SAGAX*) ABUNDANCE TO CLIMATE-SCALE ECOLOGICAL CHANGES IN THE CALIFORNIA CURRENT SYSTEM

JERROLD G. NORTON
Environmental Research Division
Southwest Fisheries Science Center / NMFS
1352 Lighthouse Avenue
Pacific Grove, California 93950
Jerrold.G.Norton@noaa.gov

JANET E. MASON
Environmental Research Division
Southwest Fisheries Science Center / NMFS
1352 Lighthouse Avenue
Pacific Grove, California 93950

ABSTRACT

Empirical orthogonal function (EOF) analyses link sardine abundance to large-scale processes of the California Current ecosystem. These analyses of the California fish and invertebrate landings (CACom) detect two patterns of variability (EOF1 and EOF2), which indicate that climate-scale changes in CACom species composition occurred during 1930–2000. California sardine landings are related to EOF1 (nominal correlation coefficient, $r' > 0.9$), linking fluctuations in sardine abundance to many other California Current species. $\log_e$-transformed sardine landings are closely related ($r' > 0.9$) to accumulated sea surface temperature anomalies at La Jolla, California and to accumulated equatorial process indices ($r' \geq 0.8$). We found that the length of time that physical anomalies persist is related exponentially to the effects these physical processes will have on sardine abundance. When the sardine series is extended backward to 1890, using sardine-scale deposition rates as an abundance proxy and the equatorial indices as physical proxies, the relationships between sardine abundance and the physical environment holds ($r' \geq 0.8$).

INTRODUCTION

The abundance of California sardines, or pilchards, (*Sardinops sagax*) off the west coast of temperate North America fluctuates, and in the 1930s and 1940s sardine populations were the source of the largest fishery of the western hemisphere (Marr 1960; Jacobson and MacCall 1995; Norton and Mason 2003). The largest landings of sardines were in California ports, where shore-based landings exceeded 400,000 metric tons (t) in each year from 1934 to 1944. California sardine populations declined sharply in the later 1940s and continued to decline into the early 1970s when annual landings were less than 10 t (Mason 2004). In 1967, a moratorium was placed on the directed California sardine fishery, but 15% by weight was allowed in mixed-species landings. In 1969, landings for dead bait were limited to 227 t, and in 1974 recovery plans were developed to allow a directed fishery of 907 t when the California spawning population was estimated to be more than 18,144 t. Increases in the harvest quota would be allowed if the spawning population continued to increase (Conser et al. 2004). In the late 1970s and 1980s, the California sardine population increased due to environmental changes (Jacobson and MacCall 1995), and their landings increased from 388 t in 1986 to more than 56,000 t in 1999 and 2000 (Mason 2004).

California state laws require that all sales of fish and invertebrates from primary harvesters (fishers) to fish dealers include the species (or species groups) and weight landed on the sales receipts. The summaries of these sales receipts for catches within the California Fishers Harvest Environment (CFHE), tabulated by the California Department of Fish and Game, were converted to Internet accessible formats by the Pacific Fisheries Environmental Laboratory (http://www.pfeg.noaa.gov/products/las.html). These records (CACom) provide information about the availability of the commercially important components of the California Current System (CCS) ecosystem (Norton and Mason 2003, 2004).

Empirical Orthogonal Function (EOF) analysis of these records showed that EOF1 and EOF2 explained more than 45% of the variance in composition of 29 species that made up more than 85% of the total CACom landings throughout the 1930–2000 period. When time-varying coefficients (principal components) of these EOFs, C1 and C2, were compared to indices of physical change in the CFHE and to time series representing fishing effort and market factors, they were found to be more closely correlated to the environmental indices than to fishing effort or market indices. Landings composition changes shown by C1 were closely related to persisting anomalous conditions in the CFHE as indicated by several physical environmental data series, including sea surface temperature (SST) measured at La Jolla, California (Norton and Mason 2003).

The purpose of this study is to investigate the relationship of sardine landings to the physical and biological environments of the CFHE, which is that part of the CCS extending from the coast of California to 400–600 km offshore between 32.5° and 42°N latitude (Norton and Mason 2003). We build on the observations that the $\log_e$ of California sardine landings weight is strongly related to C1 (Norton and Mason 2004) and

that sardine abundance in the CFHE may be indexed by SST at La Jolla, California (Marr 1960; Jacobson and MacCall 1995; MacCall 1996; and Norton and Mason 2003, 2005). We also use proxy sardine abundance records and reconstructed physical variables to investigate the relationship between physical and biological parameters in the late 1800s, before the development of the industrial sardine fishery. Anchovy abundance series are examined to show that they differ significantly from sardine landings series throughout the 1900s.

METHODS

The 29 species selected for analysis (tab. 1) were: 1) identified unambiguously by species in the landings records and 2) recorded in the catch in 60 or more of the 71 years studied (Norton and Mason 2003, 2005). Each of the 29 single-species landings records from 1930 through 2000 was $\log_e$-transformed and placed as a column-vector in the data (input) matrix. The corresponding correlation matrices were formed from the data matrix and eigenvectors (proportional to empirical orthogonal functions or EOFs), and eigenvalues of the correlation matrix were computed (Norton and Mason 2004). Only EOF1 and EOF2, which 1) explain the most and second-most variance of the input matrix and 2) are significant at less than the 0.05 level (North et al. 1982), are discussed in this report. The products of the EOFs and the corresponding data matrix give the time-variable coefficients (Cn, n = 1, 2) and indicate the variation of each unique EOF through the 1930–2000 period. Each column (species) has a loading value within the EOF. The magnitude of the loading value indicates the relationship between the time variation in Cn and the time variation of that species (see below). Each Cn-series represents a mode of temporal variation characteristic of the data matrix.

Indices of climate-scale physical environmental change were derived by taking anomalies from overall time-series means. The anomaly series, X, was accumulated (integrated) through time,

$$A - X(\gamma) = \sum_{i=b}^{\gamma} X(i), \tag{1}$$

where $A - X(\gamma)$ is the accumulation of the anomaly time series X, b is the first year of the accumulation, and γ is a year between b and 2001. The accumulated series may be interpreted in terms of processes that, together, cause negative or positive anomalies (Klyashtorin 2001; Hanley et al. 2002; Norton and Mason 2003, 2004). The length of the trend indicates the time period of persistent anomaly, and the rise of the trend indicates the magnitude of the anomalous integrated period. Seasonal and many in-

terannual events may be attenuated in these integrated indices, making accumulated series valuable for illustrating climate-scale (8–30 years) changes. These anomaly accumulation methods (Equation 1) were used to derive the first six of the eight index series described below.

First, the La Jolla A-SST climate index is derived from monthly mean SST taken at the Scripps Institution of Oceanography pier in La Jolla, California (32.9°N, 117.3°W). These SST data are available from <ftp://ccsweb1.ucsd.edu/pub/shore>.

Second, the A-SWS (southward windstress) climate index was computed for an area off Central California with consistently large numbers of observations in the Comprehensive Ocean-Atmosphere Data Set (COADS). This area is bounded by the California coast and 39°N, 124°W; 37°N, 124°W; 37°N, 123°W, and 36°N, 123°N (Parrish et al. 2000; Norton and Mason 2003). By convention, greater SWS is indicated by larger magnitude negative index values.

Third, the A-DSLP sea-level atmospheric pressure index for Darwin, Australia (12.4°S, 130.9°E) is related to El Niño-like physical events in the equatorial and CFHE regions (Norton and McLain 1994; Alexander et al. 2002; Fu and Qui 2002). Darwin SLP is available from Kousky (2003) at <http://www.cpc.ncep.noaa.gov>.

Fourth, the A-JMA index was computed from the average equatorial SST anomaly from the area defined by 4°N to 4°S, 150°W to 90°W and known as the JMA ENSO index (Hanley et al. 2002). It is available at <http://www.coaps.fsu.edu/~legler/jma_index1.shtml>.

Fifth, the A-NINO3.4 climate index was formed by accumulating deviations from the linear trend of SST anomalies in the NINO3.4 area (5°N to 5°S, 170°W–120°W). Kaplan et al. (1998) used the United Kingdom Meteorological Office historical SST data set, optimal interpolation, and other statistical techniques to reconstruct the major features of the global SST field from 1856–1991. Updated data are available from <http://ingrid.ldeo.columbia.edu/SOURCES/.Indices/.nino/.EXTENDED/>.

Sixth, the Palmyra A-cST was calculated from a 1860–1998 temperature time series derived from cores of living and fossil coral at Palmyra Island (6°N, 162°W), about 100 km north of the NINO3.4 area. This series is included because these proxy records appear to give annual measurements of shallow water sea temperature (Cobb and Charles 2001; Cobb et al. 2003). The coral record is independent of the NINO3.4 reconstruction and potentially provides estimates of sea temperature extending centuries into the past (Cobb and Charles 2001; Cobb et al. 2003). These data are available from <http://www.ngdc.noaa.gov/paleo/pubs/ cobb2003/>. Palmyra A-cST, was formed by accumulating deviations from a linear trend.

Seventh and eighth, estimates of sardine and anchovy abundances from 1850–1970 were obtained from scale-deposition rates (SDRs) in the anaerobic sediments of the Santa Barbara Basin (34.25°N, 120.09°W). Soutar and Isaacs (1974) found that these SDRs were proportional to estimates of sardine and anchovy biomass. We used the SDRs per 1000 cm^2 yr^{-1} averaged for 10-year periods (fig. 4 in Baumgartner et al. 1992,). All sardine and anchovy series are $\log_e$-transformed and, like C1 and C2, may reflect the integration of environmental anomalies, but they are not accumulated or integrated variables.

Landings Abundance and Biomass Estimates

To examine the relationship between California landings and biomass estimations for the entire West Coast stock, we compared estimated biomass for one-year-old and older fish (Conser et al. 2004) to records of sardine landings in California ports (Norton and Mason 2003; Mason 2004) for the 1932–2000 period. When each series was $\log_e$-transformed, there was a high degree of similarity between them (the nominal correlation coefficient, $r' = 0.88$). Correlation between the transformed estimated biomass and landings series was $r' = 0.77$ for the largely unregulated 1932–63 period and $r' = 0.97$ for the regulated 1983–2000 period. The major differences in the 1932–63 records occur during events shorter than eight years. The transformed landings values for the 1983–2000 period are expected to vary with the transformed biomass estimates, since landing quotas were directly dependent on biomass estimations (Conser et al. 2004). The low-abundance 1964–82 years were not included in the correlation analysis because biomass estimations are not available for this period (Jacobson and MacCall 1995).

All time series are graphed and manipulated as standardized variables (Is),

$$Is = (S - Ms) / SDs, \qquad (2)$$

where S is a discrete value in series s, Ms is the mean of s. and SDs is the standard deviation of s.

Relationships between physical and biological variables were examined graphically and by simple correlation. All correlations were tested for effective degrees of freedom (n), determined by the long-lag (20%–30%) correlation method (Chelton 1983). Herein, correlation coefficient magnitudes larger than 0.8 ($|r| > 0.8$) test by n to occur by chance at a rate of less than one in 20 trials ($p < 0.05$), but caution should be applied to this interpretation. A persisting problem with climate research on modern data is that it is undertaken with series of only a hundred-years, and any phenomena investigated will have few repetitions. The prospect for hypothesis testing using common statistical techniques is limited for
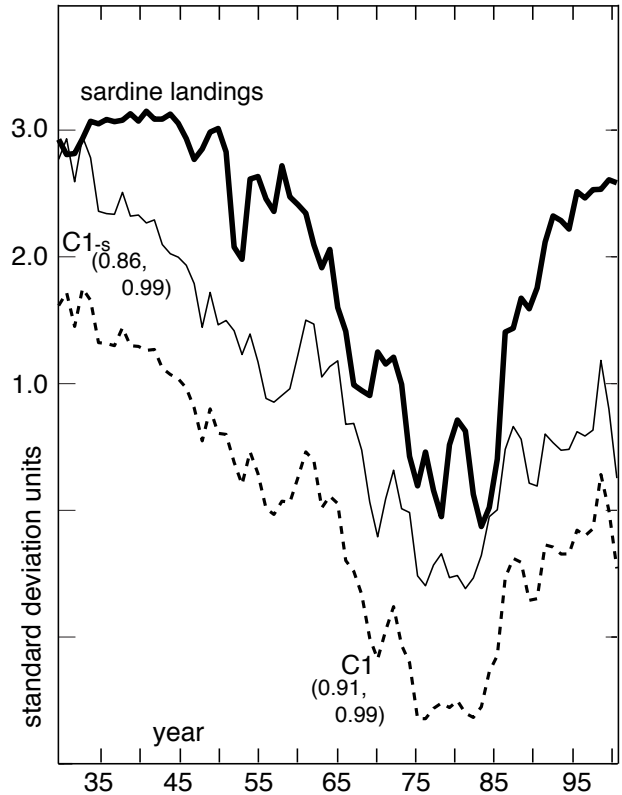

Figure 1. Sardine landings variability through the 1930–2000 period is shown by the upper, heavy line. The lower, broken line gives C1, the time variation of EOF1, derived from 29 species. The middle series, C1-s, is the same as C1 except the sardine series has been omitted from the computation (solid line). Correlation to the sardine series is given first in parentheses, and the correlation with the other variable second. C1 is closely related to the sardine landings series ($r' = 0.91$) and is nearly independent of the sardine landings series. All series are standardized and offset for comparison.

these data (von Storch and Navarra 1995). Consequently, the correlation coefficients (r'-values) are to be considered primarily as comparative statements, rather than as consistently suitable for statistical interpretation.

RESULTS

The total catch of sardines during 1930–2000 exceeded 8 million t and was close to the catch of all other species combined. Therefore, it might be expected that the sardine landings pattern would dominate the time variation in C1. However, this is not the case (fig. 1), because C1-s computed without the sardine series is nearly identical to C1 computed with the sardine series. Both are similar to the sardine series ($r' > 0.85$), indicating that many of the other 28 species used in calculating C1-s are affected either positively or negatively by the same environmental factors that affect sardine abundance (fig. 1).

Species Associations

Each of the 29 species used to calculate EOFs had periods of relatively high landings (maxima) during the
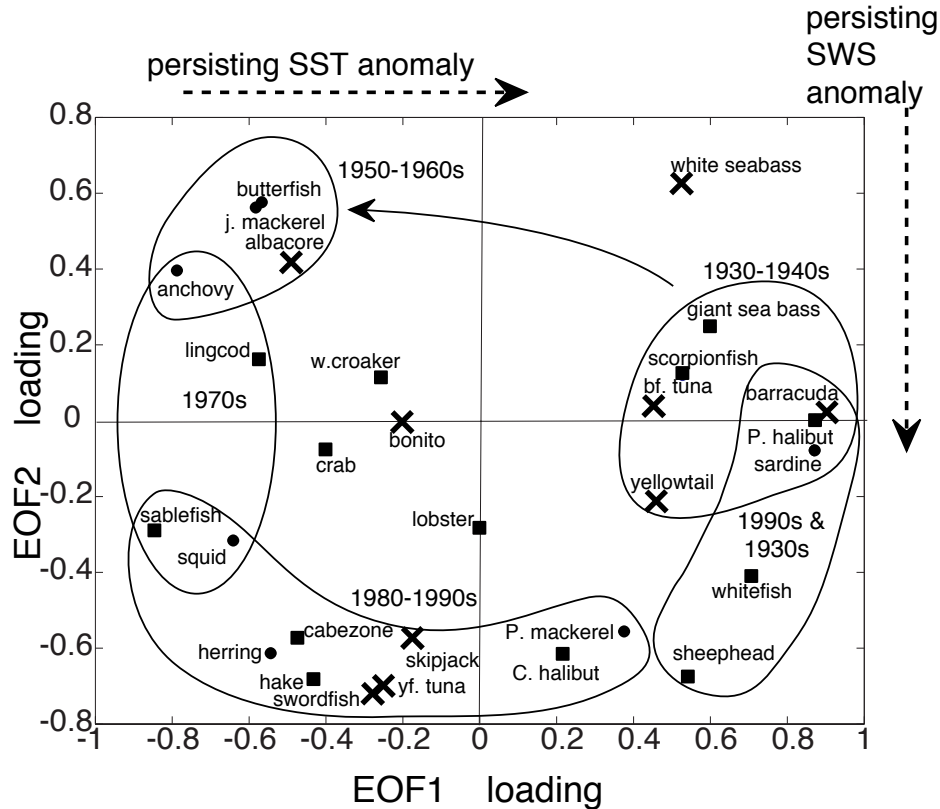
Figure 2.   Loading values are plotted for EOF1 on the horizontal and for EOF2 on the vertical axes. The enclosed species-groups show the counter-clockwise progression of species having landings maxima. Filled squares show species that are harvested from demersal habitats. Crosses indicate migratory species that are also found outside the California fishers harvest environment (CFHE), and filled circles indicate species harvested from pelagic habitats. Shifts in availability and harvest of the 29 species caught throughout the 1930–2000 period show the ecological climate signal. The dotted arrow at the top shows the shift in CFHE species composition as positive SST anomalies accumulate. The dotted arrow on the right side shows the shift in species composition as southward wind stress off California continues to be anomalously strong. By convention, southward wind stress is negative. Complete species names are given in Table 1.

1930–2000 period. The temporal distribution of characteristic species-group maxima is shown in Figure 2 (enclosed), where EOF1 loading values for each species are plotted on a horizontal axis, and EOF2 loading values are plotted on the vertical axis. Sardines, scorpionfish, barracuda, and yellowtail and Pacific mackerel were all at or near their landings maxima during the 1930s and 1940s (center right in fig. 2). Jack mackerel and albacore were near their maximum landings in the 1950s and 1960s (upper left). Anchovy and sablefish were near their maximum abundance in the landings during the 1970s (center left). Skipjack, yellowfin tuna, swordfish, hake, and Pacific mackerel were at their maximum landings during the 1980s and 1990s (lower center). A cycle appears to have completed in the 1990s (lower, right) with sheephead, whitefish, and sardines increasing in abundance. While commercial landings of barracuda and white seabass were low because of extensive regulation during the 1990s, recreational catches of barracuda and white seabass increased through this warmer period. These changes in species-group maxima may in-

dicate repeating changes in the flow of productivity (renewable food energy initially provided by photosynthesis) through the web of CCS ecological processes.

Each of the 29 species shown in Figure 2 is categorized by capture habitat: demersal, migratory, or pelagic (tab. 1). These groups are not entirely exclusive. The distribution of each habitat group through each quadrant and into four of the five species-groups (enclosed in fig. 2) shows that the climate effects found in the landings series are wide-spread in the CFHE and not limited to specific habitats.

Physical Forcing

Studies have shown that C1 is related to the large-scale patterns of physical variation that are monitored by the SST at the Scripps Institution of Oceanography pier (La Jolla) in southern California and by equatorial indices of climate variation (Norton and Mason 2003, 2004). The implication of these large-scale relationships (fig. 3) is that in the absence of mid-latitude indices, equatorial indices are suitable for monitoring the same

TABLE 1
**Harvest Habitat for 29 Species Recorded in
California Landings 1930–2000**

Demersal	n[a]
California (C) halibut[b]	*Paralichthys californicus*
cabezon	*Scorpaenichthys marmoratus*
crab	*Cancer magister*
white (w) croaker	*Genyonemus lineatus*
giant sea bass	*Stereolepis gigas*
hake	*Merluccius productus*
lingcod	*Ophiodon elongatus*
lobster	*Panulirus interruptus*
Pacific (P) halibut	*Hippoglossus stenolepis*
sablefish	*Anoplopoma fimbria*
scorpionfish	*Scorpaena guttata*
sheephead	*Semicossyphus pulcher*
whitefish	*Caulolatilus princeps*
Migratory[c]	**x**
albacore	*Thunnus alalunga*
barracuda	*Sphyraena argentea*
bluefin (bf) tuna	*Thunnus thynnus*
bonito	*Sarda chiliensis*
skipjack	*Euthynnus pelamis*
swordfish	*Xiphias gladius*
white seabass	*Atractoscion noblis*
yellowtail	*Seriola dorsalis*
Yellowfin (yf) tuna	*Thunnus albacares*
Pelagic	**c**
anchovy	*Engraulis mordax*
butterfish	*Peprilus simillimus*
herring	*Clupea pallasi*
Jack (j) mackerel	*Trachurus symmetricus*
Pacific (P) mackerel	*Scomber japonicus*
sardine	*Sardinops sagax*
squid	*Loligo opalescens*

[a]Symbol used in Figure 2 for this harvest group.
[b]Naming conventions follow those of Miller and Lea (1972).
[c]Indicates species that migrate into the CFHE, but are not generally present throughout the year.
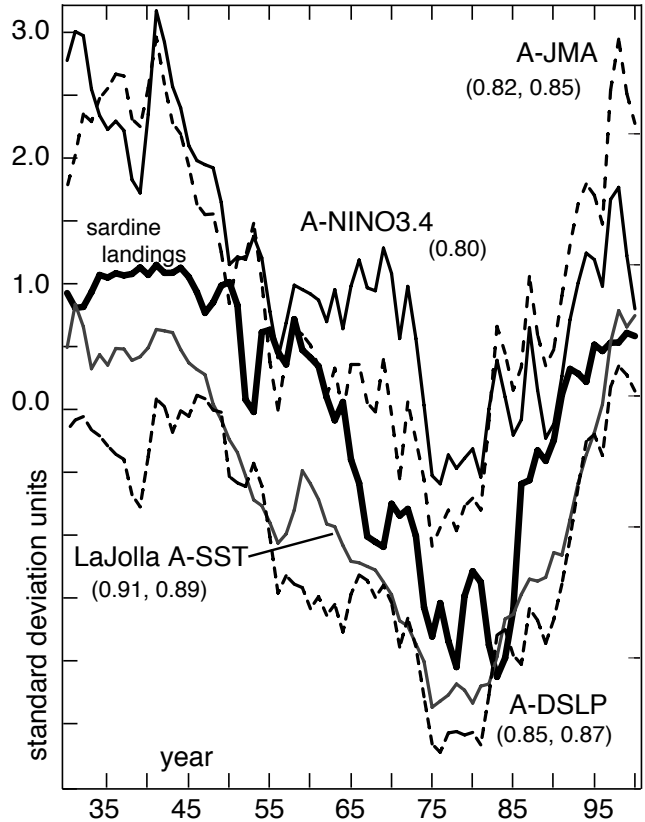

Figure 3.   Comparison of sardine landings (heavy, solid line) to physical indices from southern California (La Jolla A-SST, lower, solid line) and the equatorial atmosphere-ocean system. Numbers in parenthesis show correlations first to the sardine series and second to the A-NINO3.4 series (upper, solid line). A-JMA (upper, broken line) and A-NINO3.4 represent the SST anomaly over large areas of the equatorial ocean (see Methods). A-DSLP is shown by the lower, broken line. All series are standardized and may be offset for clarity.

large-scale phenomena that appear to regulate sardine abundance and 30% of the variability in commercial fish landings from the CFHE.

Changes in La Jolla SST are correlated with 1000 kilometer-scale ocean events in the eastern temperate Pacific (Marr 1960; McGowan et al. 1998; Norton 1999). The Darwin sea–level pressure indexed by A-DSLP and the equatorial SST indexed by A-JMA and A-NINO3.4 are unambiguous representations of equatorial climate events. The remote climate signal is clearly represented within the CFHE by the La Jolla A-SST, which is more closely related to sardine abundance than the equatorial indices during 1930–2000. It is clear from Figure 3 that on climate scales of eight to 60 years, there is considerable correlation of physical variability ($r' \geq 0.80$) throughout the equatorial and northeastern Pacific, which is also correlated to sardine abundance.

If the CFHE sardine stocks are as extensively utilized and sampled as they were throughout most of the 1930–2000 period then,

$$\log_e (B) = f(s) \sum (A), \qquad (3)$$

where B is the abundance measure in weight, A is the environmental process anomaly and $f(s)$ is a scaling function. Herein, $f(s)$ represents standardization (Equation 3). If the La Jolla A-SST, as shown in Figure 3, represents the right side of Equation 3, then its values would be the calculations of $\log_e$ sardine abundance (fig. 3, La Jolla A-SST), and the correlation between the observed (fig. 3, sardine landings) and calculated would be $r' = 0.91$ for the 1930–2000 period. Equation 3 expresses an exponential biological response, shown in sardine abundance and C1, to the processes represented by the accumulating anomaly.

Of the equatorial indicators, A-DSLP appears most closely related to sardine abundance ($r' = 0.85$). The A-JMA and A-NINO3.4 appear less closely related to sardine abundance ($r' \geq 0.80$), but the overall pattern of these two equatorial SST variables is similar to the others shown in Figure 3. The close correspondence in
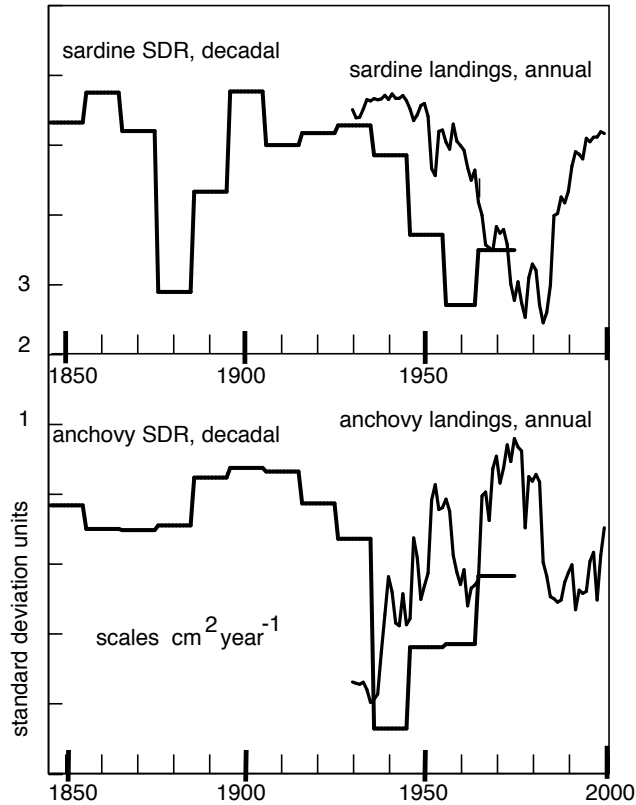
Figure 4.   The upper panel shows comparison of sardine abundance estimates from scales (heavy, stepped line) and sardine abundance estimates from the California commercial landings (CACom). The lower panel compares estimates of anchovy abundance from scale deposition rates (SDR) with the CACom landings of anchovy. Each series is $\log_e$-transformed before standardization. Scale abundance estimates are from scale deposition rate in number of scales per 1000 cm^2 $year^{-1}$ (SDR).

turning points and the length of the periods of positive and negative anomaly (positive and negative slope) show that the decadal changes in the California Current region are basin scale and may be detected in equatorial processes. The A-JMA and A-NINO3.4 equatorial indices are rich in one to seven year (interannual) variability. Much of this variability is reflected one to four years later as fluctuations in sardine landings (e.g., 1950–56 and 1975–83 in fig. 3), suggesting an equatorial to CFHE influence on these timescales, as well as on climate scales that are the focus of this report.

Extending the Biological Series

Baumgartner et al. (1992; fig. 4) present time series from 500 to 1970 of sardine and anchovy abundance based on their scale-deposition rates (SDR) in the anaerobic sediments of the Santa Barbara Basin. If the sardine SDR can be used to examine how physical events correspond to sardine abundance, then SDR series provide comparisons that will be independent of previous tests based on the 1930–2000 CACom landings.

The decadal $\log_e$-transformed SDRs are compared to the annual $\log_e$-transformed sardine and anchovy landings in Figure 4. SDR series are centered on the decade indicator (e.g., 1940, 1950, etc.). Both sardine series show a decline in the 1930–70 period. The greatest rate of decline in sardine landings occurred during 1956–65, an interval when few sardine scales were deposited. After the sharp decline of the 1960s, there was a small increase in both sardine series, possibly related to the 1972–73 El Niño period when local reproduction and migration from the south were enhanced. For the anchovy series, there is an increase in landings in two steps through the 1930–70 period. Differences in lead–lag dynamics between the landings and scale sedimentation lead to the differences between the SDR and landings series (e.g., sardine in the 1930s, fig. 4). However, the general agreement between landings and SDR series (fig. 4) and the findings of Soutar and Isaacs (1974), who found proportionality between SDR and biomass estimates of sardine and anchovy for the 1930–58 period, indicate that the SDR series may be a usable proxy for CFHE sardine and anchovy abundance.

Extending the Physical Series

Four physical series are compared over their common ranges (fig. 5) to examine the possibility of extending the physical series backwards. The NINO3.4 reconstruction is the longest, extending from 1856 to the present. The Palmyra A-cST, A-DSLP, and La Jolla A-SST indices extend back from 2000 to 1886, 1890, and 1917, respectively (fig. 5). There is generally good agreement among the physical indices back to about 1910 (fig.5). A-NINO3.4 has greater amplitude variability causing divergence at several scales throughout the record. However, the phase of interannual events is similar in each series.

Scale Deposition Compared to Physical Variability 1890–1970

The equatorial indices, found to be reasonable proxies for CFHE climate processes, and the sardine SDR record of Baumgartner et al. (1992) are compared in Figure 6. The four physical series are fundamentally similar; they are different estimations of the same climate events detected at different locations. For clarity, the A-cST time series is not shown, but, for comparison, r'-values for A-cST appear in Figure 6 below the r'-values for A-DSLP.

The sardine-scale records approximate 10-year SDR averages (Baumgartner et al. 1992). The physical data represent annual estimates of climate-scale environmental processes. Generally, scale deposition and the physical environment were more correlated when compared by the center annual physical values (e.g., 1910, 1920, etc.) than when compared by averages of the ten annual
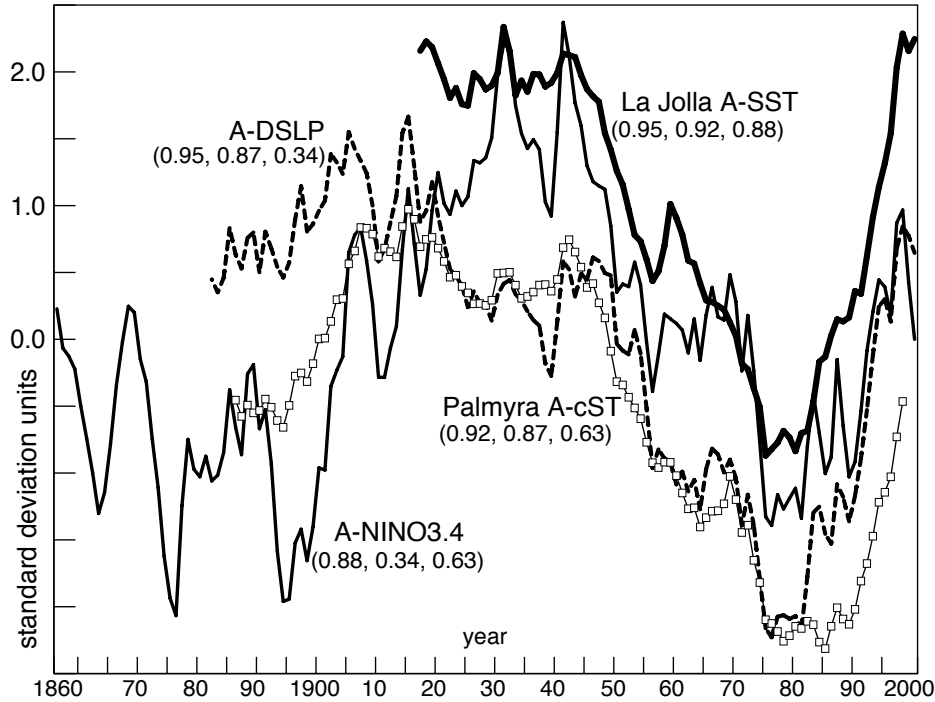
Figure 5. Indices of climate-scale changes from the sea surface temperature for southern California (La Jolla A-SST, heavy, top line); Darwin sea level atmospheric pressure (A-DSLP, broken line); sea temperature derived from coral at Palmyra Island (Palmyra A-cST, open squares); and SST reconstruction for the NINO3.4 equatorial area (A-NINO3.4, lower, solid line). Correlation coefficients appear beneath each series label. From left to right they give coefficients for that series correlated with La Jolla A-SST, A-DSLP, Palmyra A-cST, and A-NINO3.4, excluding the labeled series. All series are standardized and may be offset for clarity. After 1920, the series diverge but show many of the same higher frequency events.

values of the 10-year period. Center-of-the-decade annual values are used throughout the following discussion. Algorithms that allow for temporal errors and find the best fits while allowing temporal error windows will be developed and compared in future reports.

For the 1930–2000 period there is an inverse correlation between sardine and anchovy abundance as measured by the California commercial landings (figs. 2, 4), but the abundance of one species has an orthogonal relationship with the abundance of the other (vertical scale in fig. 2). If Equation 3 is appropriate for the backward extended series, then the orthogonal relationship may cause the anchovy SDR series to be less correlated to the physical indices shown in Figure 5. This will be a test for the particularity or lack of randomness in the two series. When the sardine-scale record is compared to the physical variables for 1920–70, correlations greater the 0.80 are found for all variables (fig. 6). None of the physical variables are strongly related to the anchovy-scale series (not shown). The hypothesis presented by Equation 3 is supported by its relationship to the sardine series and by its lack of relationship to the partially orthogonal anchovy series.

When the 1890–1970 period is considered, A-DSLP and Palmyra A-cST are highly correlated with sardine SDR (0.85 and 0.89, respectively) (fig. 6, second line beneath variable labels). The correlations of these variables with the anchovy-scale SDR increase to 0.58 and 0.20, respectively, but these r'-values continue to indicate distinct differences between the sardine and anchovy correlations.

During 1860–1920, the A-NINO3.4 and sardine SDR series are visually similar to those encountered during 1920–70, but the r'-values do not reflect these similarities because of accumulated aging inaccuracies in the sardine SDR series (fig. 6). For example, the 1895–1907 period corresponds to the highest sardine SDR in the entire 1860–2000 period and to some of the lowest A-NINO3.4 values. However, the longest period of sustained high-value positive anomalies (sustained, high-value slope) for NINO3.4 corresponds to the high SDR values. Better reconstructions of the NINO3.4 SST anomaly and a more complete development of high temporal resolution, coral-derived sea temperature will likely improve our ability to derive past relationships between sardine abundance in the CFHE and large-scale physical processes. Although the SDR series appears limiting, there is large potential for improving it.

The backward extension of the relationships between sardine abundance and physical variables augments the
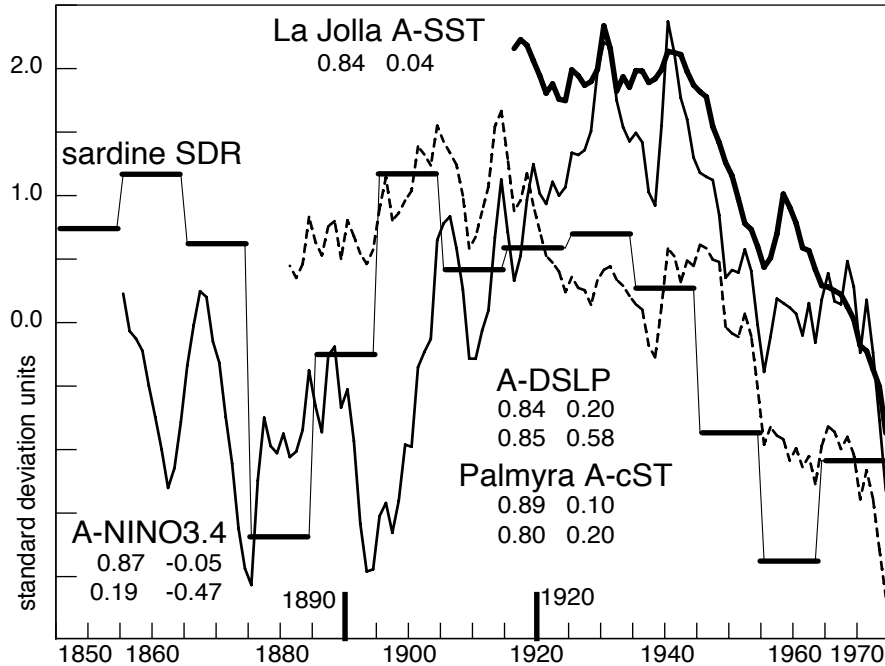
Figure 6. Comparison of decadal average sardine-scale deposition rates (heavy, stepped line) to physical climate variables: accumulated SST anomaly from southern California (La Jolla A-SST, upper, solid line); accumulated sea level atmospheric pressure northern Australia (A-DSLP, broken line), and accumulated SST anomaly in the NINO3.4 area of the equatorial ocean (A-NINO3.4, lower, solid line). The correlation of the scale deposition (SDR) to the physical variables is given below each label, sardine-left and anchovy-right. The anchovy series is not shown. The top two r'-values are for the 1920–1970 period and the lower two r'-values are for the 1890–1970 period. Because of its similarity to A-DSLP, the accumulated coral sea temperature anomaly (Palmyra A-cST) series is not shown, but its correlations to the sardine and anchovy scale series are shown beneath A-DSLP r'-values. All series are standardized and may be offset for clarity.

hypothesis that was formed using sardine landings for the 1930–2000 period (Equation 3); Log_e of sardine abundance is proportional to the time integral of environmental anomalies. The relationship shown in Figure 6 extends the test periods to include 110 years and satisfies conditions of a test independent of the CACom landings series. Extending the series forward to include the 2001–05 period will also provide hypothesis tests, but management and market effects will have to be addressed in this interval. Sardine harvest quotas have been set for each year from 2001 to 2005 by the Pacific Fisheries Management Council, but these quotas have not always been landed. We will discuss this period in future reports.

DISCUSSION

Problems arise when dealing with data from only a few decades when decadal-scale phenomena are investigated. However, three factors suggest that we have found major modes of physical-to-biological interaction: 1) the physical variables suggest relatedness by their similarity to both sardine and C1 variability; 2) the similarity of sardine and C1-s variability suggests that the physical factors affecting sardine abundance also affect the abundance of many other species; and 3) similar re-

sults were obtained using SDRs as independent estimates of sardine abundance.

Sardine Abundance and Utilization

Extensive use of CFHE fish and invertebrate resources was promoted by increasing the consumption of fish and fish products locally and by exploitation of world markets by California fish dealers (Wolf et al. 2001; Dietz et al. 2003; Norton and Mason 2004). If the fish population is larger, then the catch will be larger when there is extensive utilization and demand, particularly in unregulated fisheries tied to global markets (Dietz et al. 2003; Norton and Mason 2004). The landings series for sardines appears to be a reasonably good proxy for sardine abundance in the 1930s through the 1950s because of the high exploitation rate of about 40% of sardines 3 years old and older through 1965. Exploitation may have been even higher relative to the low population levels in the 1960s and 1970s (MacCall 1979). The recovery period of the 1980s and 1990s was managed for an exploitation rate of 15% or less (Conser et al. 2004); landings totals are directly proportional to biomass estimates ($r' = 0.97$, for log_e-transformed series) for this period.

In many cases, biomass estimates using available abundance-related indices are better measures of popu-

lation abundance than California landings, even though biomass estimated for the same time period from multiple indices may vary by 20% or more from one estimation model to another (Conser et al. 2004). However, landings time-series values may change in minor ways as new records are discovered. The record keeping of the California Department of Fish and Game (Mason 2004) has created stable and largely unchanging California sardine landings series that are proportional to state-of-the-art biomass estimates of abundance ($r' = 0.88$, for $\log_e$-transformed series).

When the resource is extensively utilized, economic factors become less important and physical environmental changes contribute more to variability as shown by sardine landings and C1. However, the extent of utilization only affects the present study when landings records are used as indicators of resource abundance (Norton and Mason 2004).

Before the early 1930s, the sardine scale deposition rates (SDR) indicated abundance better than landings because the sardine populations were not extensively utilized. The implication of the relationship between the sardine SDRs and the physical variables (fig. 6) is that the population was larger before and during the development of the industrial fishery in the 1920s than the 1930s and 1940s. It is possible that the continued development of the industrial fishery in the 1930s and 1940s depressed the sardine population to the point of marginal replacement even during these times of good growth and reproduction (sardine SDR, fig.4). When the ocean climate changed in the 1950s, the population reduced rapidly because the sardine population weight responds exponentially to sustained environmental anomalies (Equation 3).

Overall, sardine abundance depends as heavily on the ongoing physical processes, which account for 60–80% of the variability, as any other factor. When 29 species are considered together, physical processes related to C1 and C2 account for about 45% of the overall ensemble variance. Anthropogenic, ecological, and other environmental factors not represented by environmental indices account for more than 50% of the overall variance of the 29 species matrix (see also Norton and Mason 2003, 2005).

A 50–70 year cycle is shown in Figure 2, and similar cycles appear in fisheries and physical variables throughout the northern hemisphere (MacCall 1996; Klyashtorin 2001). Sixty-year cycles are also a dominant mode of temporal variability in the Baumgartner et al. (1992) SDR series. It is likely that much of the California Current ecology is cycling through variable ecosystem composition in 50-to-70-year temporal modes (e.g., fig. 2). If this is the case, then the sardine population biomass may be an indicator of many less conspicuous aspects of the ecosystem.

Ecosystem Management and Prediction

There are two ways that the relationships summarized by Figures 1, 2, 3, and 6 and Equation 3 might be used in management to obtain large yields in favorable growth environments (e.g., 1900–30) and smaller protective yields in unfavorable growth environments (e.g., 1950–75). These are persistence and ecosystem knowledge. From the SDR records of Baumgartner et al. (1992) and present studies, we show that periods of good sardine growth and periods of poor sardine growth are persistent. Management agencies might be especially alert to downturns in sardine production after a few decades of growth and abundance.

Each year there is more ecosystem information to apply to fisheries management. Following the leads of Marr (1960), Jacobson and MacCall (1995), MacCall (1996), and Parrish et al. (2000), we have shown some major physical environmental changes of the CFHE that are associated with high and low sardine production. Persisting anomalies in the environmental indices given herein will be associated with changes in sardine reproduction and recruitment. Current sardine management plans recognize some of these environmental connections, particularly the SST at La Jolla (Conser et al. 2004), but there is ample room for refining management inputs.

There are also predictive possibilities. When sardines are present, favorable environmental conditions are rapidly converted to increased sardine population biomass. The population's increase in weight will then be converted into increases in gametes and possibly recruits. An increase in individuals will depend on the continuing overall adequacy of the environment. Sardine condition and the recruitment-environment indices presented will indicate the continuity within the context of the physical relationships and independent stock assessments. Further investigations into lead–lag relationships among species are likely to show that there are species whose increase or decline regularly precedes sardine abundance changes. Changes in the availability of associated species and strong resurgence of species that do well in conditions different than sardines do (fig. 2, negative EOF1 loading) indicate that ecological changes are occurring. These ecological forewarnings may be used to assess the likelihood of sardine population growth and assist fisheries management decisions.

CONCLUSIONS

The test of the hypothesis that the accumulation of physical process anomalies is directly proportional to an exponential change in sardine abundance (Equation 3) was extended from 71 to 111 years using proxy records of sardine abundance and equatorial measurements of large-scale Pacific processes affecting the California

Current environment. This is a 40-year extension of the sardine abundance time series into the period before the sardine industrial fisheries were developed. The sardine series extension would not have been possible without scale deposition records, since sardine landings weights were relatively small compared to the estimated California Current biomass and may not reflect abundance before 1930. If our results continue to be confirmed, they will allow management decisions based on knowledge of current and probable future fluctuations in sardine and other fishery resources.

There are three related results. First, there are relatively low noise levels in the averaged sardine landings and other landings data. This is shown by the large percentage of variance in sardine landings (60–80%) and in ensemble landings matrices (40–50%) explained by physical variables.

Second, the progression of sardine landings and other species landings maxima appears tied to environmental and ecological conditions that appear to have completed a 50–70 year cycle and returned in the 1990s to physical and biological conditions similar to those of the 1930s and 1940s. Extending the record backward, we note that the conditions of 1980s and 1990s prevailed through the previous high sardine growth and abundance period of late 1800s and early 1900s.

Third, the relationships presented in this report imply that fluctuations in California Current sardine abundance within the 1880–2000 period were as dependent on measurable large-scale physical processes as on anthropogenic factors during all sub-intervals.

ACKNOWLEDGMENTS

LITERATURE CITED

Alexander, M., A. I. Bladé, M. Newman, J. R. Lanzante, N.-G. Lau, J. D. Scott. 2002. The atmospheric bridge: The influence of ENSO teleconnections on air-sea interaction over the global oceans. J. Climate. 15:2205–2231.

Baumgartner, T. R., A. Soutar, and V. Ferreira-Bartrina. 1992. Reconstruction of the history of Pacific sardine and northern anchovy populations over the past two millennia from sediments of the Santa Barbara Basin, California. Calif. Coop. Oceanic Fish. Invest. Rep. 33:24–40.

Chelton, D. B. 1983. Effects of sampling errors in statistical estimation. Deep-Sea Res. 30 (10A):1083–1103.

Cobb, K. M., C. D. Charles. 2001. A central tropical Pacific coral demonstrates Pacific, Indian, and Atlantic decadal climate connections. Geophys. Res. Lett. 20:2209–2212.

Cobb, K. M., C. D. Charles, H. Cheng, and R. L. Edwards. 2003. El Niño/Southern Oscillation and tropical Pacific climate during the last millennium. Nature. 424:271–276.

Conser, R., K. Hill, P. Crone, N. Lo, and R. Felix-Uraga. 2004. The coastal pelagic species fishery management plan. Portland: Pacific Fishery Management Council. 167 pp.

Dietz, T., E. Ostrom, and P. C. Stren. 2003. The struggle to govern the commons. Science. 302:1907–1912.

Fu, L.-L. and B. Qui. 2002. Low frequency variability of the North Pacific Ocean: The roles of boundary- and wind-driven baroclinic Rossby waves. J. Geophys. Res. 107:3220–3235.

Hanley, D. E., M. E. Bourassa, J. J. O'Brien, S. R. Smith, and E. R. Spade. 2002. A quantitative evaluation of ENSO indexes. J. Climate. 16:1249–1258.

Jacobson, L. D. and A. D. MacCall. 1995. Stock-recruitment models for Pacific sardine (*Sardinops sagax*). Can. J. Fish. Aquat. Sci. 52:566–577.

Kaplan, A., M. A. Cane, Y. Kushnir, A. C. Clement, M. B. Blumenthal, and B. Rajagopalan. 1998. Analyses of global sea surface temperature 1856–1991. J. Geophys. Res. 103:18567–18589.

Klyashtorin, L. B. 2001. Climate change and long-term fluctuations of commercial catches. Rome: Food and Agriculture Organization of the United Nations Fish. Tech. Paper 410, 86 pp.

Kousky, V. E., ed. 2003. Climate Diagnostic Bulletin. National Oceanic and Atmospheric Administration, National Weather Service, National Centers for Environmental Prediction, Camp Springs Maryland, 31 pp.

MacCall, A. D. 1979. Population estimates for the waning years of the Pacific sardine fishery. Calif. Coop. Oceanic Fish. Invest. Rep. 20:72–82.

MacCall, A. D. 1996. Patterns of low-frequency variability in the California Current. Calif. Coop. Oceanic Fish. Invest. Rep. 37:100–110.

Marr, J. C. 1960. The causes of major variations in the catch of Pacific sardine. *In* Proceedings of the world scientific meeting on the biology of sardines and related species, H. Rosa and G. Murphy, eds. Rome: Food and Agriculture Organization of the United Nations, pp. 667–791.

Mason, J. E. 2004. Historical patterns from 74 years of commercial landings from California waters. Coop. Oceanic Fish. Invest. Rep. 45:180–190.

McGowan, J. A., D. R. Cayan, and L. M. Dorman. 1998. Climate-ocean variability and ecosystem response in the Northeast Pacific. Science. 281:210–217.

Miller, D. J. and R. N. Lea. 1972. Guide to the coastal marine fishes of California. Calif. Dep. Fish Game Fish Bull. 157, 235 pp.

North, G. R., T. L. Bell, R. F. Cahalan, and F. J. Moeng. 1982. Sampling errors in the estimation of empirical orthogonal functions. Mon. Wea. Rev. 110:699–706.

Norton, J. G. and D. R. McLain. 1994. Diagnostic patterns of seasonal and interannual temperature variation off the west coast of the United States: Local and remote large scale forcing. J. Geophys. Res. 99:16,019–16,030.

Norton, J. G. 1999. Apparent habitat extensions of dolphinfish (*Coryphaena hippurus*) in response to climate transients in the California Current. Sci. Mar. (Barc.). 63:239–260.

Norton, J. G. and J. E. Mason. 2003. Environmental influences on species composition of the commercial harvest of finfish and invertebrates off California. Calif. Coop. Oceanic Fish. Invest. Rep. 44:123–133.

Norton, J. G. and J. E. Mason. 2004. Locally and remotely forced environmental influences on California commercial fish and invertebrate landings. Calif. Coop. Oceanic Fish. Invest. Rep. 45:136–145.

Parrish, R. H., F. B. Schwing, and R. Mendelssohn. 2000. Mid-latitude wind stress: the energy source for climatic shifts in the North Pacific Ocean. Fish. Oceanogr. 9:224–238.

Soutar, A. and J. D. Isaacs. 1974. Abundance of pelagic fish during the 19th and 20th centuries as recorded in anaerobic sediment off the Californias. Fish. Bull., U.S. 72:257–273.

von Storch, H. and A. Navarra, eds. 1995. Analysis of climate variability, applications and techniques. New York: Springer, 334 pp.

Wolf, P., P. E. Smith, and D. R. Bergen. 2001. Pacific sardine. *In* California's living marine resources: A status report, Leet, W. S., C. M. Dewees, R. Klingbeil, and E. J. Larson, eds. Oakland, CA: University of California Agriculture and Natural Resources SG01-11, pp. 299–302.